ERCO-Net: Enhancing Image Dehazing for Optimized Detail Retention

Muhammad Ayub Sabir[1], Fatima Ashraf[2]*, Ahthasham Sajid[3],
Nisreen Innab[4], Reem Alrowili[5], Yazeed Yasin[6]
Department of Information Technology, Beijing University of Technology, China[1,2]
Department of Cyber Security-Riphah Institute of Systems Engineering, Riphah International University, Pakistan[3]
Department of Computer Science and Information Systems-College of Applied Sciences, AlMaarefa University, Diriyah, Saudi Arabia[4,5]
Department of Computer Science and Software Engineering, Al Ain University, Al Ain, United Arab Emirates[6]

***Abstract*—Image dehazing is a crucial preprocessing step in computer vision for enhancing image quality and enabling many downstream applications. However, existing methods often do not accurately restore hazy images while maintaining computational efficiency. To overcome this challenge, we propose ERCO-Net a new fusion framework that combines edge restriction and contextual optimization methods. By using boundary constraints, ERCO-Net extend the boundaries that help in protecting the edges and structures of an image. Contextual optimization impacts the final quality of the dehazed image by enhancing smoothness and coherence. We compare ERCO-Net with conventional approaches such as dark channel prior (DCP), All-in-one dehazing network (AoD), and Feature fusion attention network (FFA-Net). The comparative evaluation highlights the effectiveness of the proposed fusion method, providing significant improvement in image clarity, contrast, and colors. The combination of edge restriction and contextual optimization not only enhances the quality of dehazing but also decreases computational complexity, presenting a promising avenue for advancing image restoration techniques. The source code is available at https://github.com/FatimaAyub12/Image-Dehazing-.**

***Keywords*—Image dehazing; edge restriction; contextual optimization; transmission map estimation; haze removal**

I. Introduction

Enhancing visibility in foggy or hazy conditions is a crucial objective in image processing, with picture dehazing playing a key role in achieving this improvement [1], [2]. Dehazing techniques improve image clarity and expose latent details by lowering the effect of ambient scattering. These methods quantify and eliminate haze-generated degradation using mathematical models while analysing pixel intensities and colours [3]. Popular techniques for enhancing image contrast and visibility include the dark channel prior [4] and atmospheric light estimation [5]. Where effective analysis and decision-making depend on clear, detailed images, dehazing finds uses in many disciplines including computer vision, surveillance and remote sensing. [6]. An illustration of a hazy image and its corresponding dehazed version is presented in the Fig. 1.

Early methods for haze reduction mostly depended on either several views of the same image or extra depth information. Notable contributions in this field are shown by several papers, including [2], [1], [3], [4]. Particles in the atmosphere partially polarise light as Schechner et al. [7] noted. The researchers used this finding to propose a method for quickly reducing haze using polarisation to take two pictures from different angles.

Fig. 1. Example of the image with haze (left) and dehazed image (right).

However, despite the advancements in this field, existing dehazing methods often struggle with maintaining a balance between image restoration quality and computational efficiency. Many of these techniques tend to either oversimplify the haze model or fail to preserve critical image details, such as edges and textures, resulting in suboptimal dehazed images with artifacts and color distortions. Furthermore, the increasing complexity of deep learning-based approaches introduces significant computational overhead, making real-time dehazing a challenging task Single image dehazing poses a challenge due to its inherent lack of complete information, making it an under-constrained problem. To address this, the conventional approach involves integrating additional priors or constraints. This paper delves into this notion by establishing an inherent boundary constraint concerning scene transmission. For the purpose of obtaining the illusive transmission parameters, an optimisation framework is constructed using this restriction alongside with a weighted L_1 norm-based contextual optimisation among neighbouring pixels. ERCO-Net operates on a set of fundamental assumptions and demonstrates the capability to produce high-quality, haze-free images with accurate color representation and intricate edge details. Summarizing, the main contributions of this paper are:

*Corresponding authors.

- Firstly, we introduce a novel constraint concerning scene transmission. This straightforward constraint, with its clear geometric interpretation, proves remarkably effective in image dehazing.
- Secondly, we propose a contextual optimization method that allows us to integrate a filter bank into the image dehazing process. These filters play a crucial role in reducing image noise and enhancing significant image features, such as abrupt edges and corners.
- Finally, we present an efficient optimization scheme, enabling rapid dehazing of large-sized images.

The remainder of this paper is organized as: Section II presents a detailed literature review, highlighting existing approaches to image dehazing. Section III introduces the proposed ERCO-Net framework, including edge restriction and contextual optimization techniques. Section IV discusses the methodology behind the edge restriction from the radiance cube and contextual regularization. Section V provides a comprehensive analysis of experimental results and a comparison with other state-of-the-art methods. Finally, Section VI concludes the paper with a summary of findings and future research directions.

II. Literature Review

The related work critically examines seminal works in image processing, atmospheric scattering models, and computational photography. It highlights the strengths and limitations of existing algorithms, emphasizing the need for novel approaches to address challenges in dehazing, such as preserving image details, handling varying haze densities, and improving computational efficiency. By synthesizing insights from diverse scholarly contributions, this review sets the foundation for proposing innovative solutions to enhance visual clarity and fidelity in hazy environments.

A. Network-Based Approaches for Image Dehazing

Convolutional Neural Networks (CNNs) play a pivotal role in modern deep learning-driven dehazing networks. These networks utilize different modules including standard convolution, dilated convolution, multi-scale fusion, feature pyramid, cross-layer connections, and attention mechanisms. Typically, these modules are combined into multiple basic blocks within a dehazing network architecture. This approach aids in comprehending the underlying principles of different dehazing algorithms. To facilitate understanding, the commonly used basic blocks in network architectures are summarized as follows.

1) Standard convolution neural network: Research has demonstrated the effectiveness of employing standard convolution in a sequential manner for constructing neural networks. Hence, it is a common practice to integrate standard convolution into dehazing models alongside other blocks [8], [9], [10], [11].

2) Dilated convolution: In Dilated Fusion, a method is used that enlarges the receptive field without changing the dimensions of the convolution kernel. Various studies [12], [13], [14], [15], [16] have shown its effectiveness in improving global feature extraction. Additionally, integrating convolution layers with varying dilation rates allows for the extraction of features from different receptive fields.

3) Multi-scale fusion: Research has shown that employing Convolutional Neural Networks (CNNs) with multi-scale convolution kernels can effectively extract features across various visual tasks. This approach utilizes convolution kernels of different scales and combines the extracted features, proving beneficial in tasks such as dehazing [17], [18], [19], [20]. Through fusion strategies, these methods achieve multi-scale details essential for image restoration. Typically, during feature fusion, output features obtained from convolution kernels of varying sizes are spatially concatenated or added together.

4) Feature pyramid: In the domain of digital image processing research, the concept of a feature pyramid emerges as a powerful tool. This pyramid allows for the extraction of information at various resolutions from an image. Within the domain of deep learning-based dehazing networks, researchers [21], [22], [23], [24], [25], [11], [26] have employed this strategy within the intermediate of the network layers. Here, the aim is to capture diverse scales of spatial and channel information, enhancing the ability of network to effectively dehaze images. The author in [27] introduces a novel transformer-based architecture for image dehazing that embeds transmission-aware information into the position encoder, addressing the challenge of varying haze densities across different spatial regions. It offers a new method of global and local feature integration for enhanced image clarity.

5) Cross-layer interconnection: To improve information exchange across different layers and strengthen the network's ability to extract features, CNNs frequently use cross-layer connections. In the domain of dehazing networks, three primary types of cross-layer connections emerge: The authors initially proposed ResNet, this approach is widely utilized in [28], [29], [30], [31], [32]. The second type, Dense Connection is applied in the works of [33], [34], [35]. While the third, Skip Connection have been integrated into various architectures [26], [36], [17], [13].

6) Attention dehazing: The attention mechanism has proven to be highly effective in natural language processing research. In the realm of computer vision, two commonly used attention mechanisms are channel attention and spatial attention. Channel attention plays a crucial role in the feature extraction and reconstruction of 2D images. It emphasizes the significant channels in a feature map, allowing the model to concentrate on essential feature details. This targeted approach boosts the efficiency of feature extraction. Meanwhile, spatial attention centers on the variations in feature positions within the map. For example, it can identify and prioritize regions with distinct characteristics, such as areas heavily affected by haze across the entire map. Integrating these attention mechanisms into neural networks has led to significant advancements in various tasks, including image dehazing. Several state-of-the-art dehazing methods [28], [37], [13], [30], [38], [39], [40], [41], [14], [23], [42], [11] have been applied by a number of advanced dehazing methods, which has greatly led to their commendable performance gains. As shown in [43], adversarial auto-augmentation techniques can improve the generalization of dehazing networks. This method adjusts haze density and distribution, allowing the network to generalize better across synthetic and real-world datasets.

The use of deep networks for image dehazing faced some challenges that include increased computational complexity

TABLE I. COMPARATIVE ANALYSIS OF IMAGE DEHAZING TECHNIQUES

Method	Key Features/Approach	Advantages	Limitations	Performance (PSNR / SSIM)
Dark Channel Prior (DCP) [44]	Atmospheric scattering model, dark channel prior used to estimate transmission map	Simple and effective for natural outdoor scenes	Fails with bright sky regions, introduces halo artifacts	16.62 / 0.817 (NHHaze)
All-in-One Dehazing Network (AoD) [8]	CNN-based approach with end-to-end learning	High computational efficiency, suitable for real-time applications	May oversimplify dehazing, causing loss of details	19.06 / 0.85 (NHHaze)
Feature Fusion Attention Network (FFA-Net) [40]	Multi-scale CNN with attention mechanisms for feature fusion	Preserves fine details, improves image contrast	High computational cost, may overfit on synthetic datasets	34.59 / 0.975 (NHHaze)
ERCO-Net (Proposed)	Edge restriction and contextual optimization, boundary constraints on transmission map	Maintains edge details, smooths transitions, reduces computational complexity	Slightly more complex than basic CNN methods	37.61 / 0.991 (NHHaze)

and possible overfitting due to high parameters' count. Moreover, sometimes deep networks do not work well enough for capturing complex atmospheric scattering effects appropriately in order to gain unsatisfactory quality in dehazed images. In contrast, employing edge restrictions and contextual optimization offers distinct advantages. These methods provide explicit guidance on preserving important image features and structural details during dehazing, ensuring more accurate and visually pleasing results. Moreover, they facilitate better incorporation of prior knowledge about haze distribution and scene characteristics, leading to improved generalization and robustness in various environmental conditions. Table I provides a comparative analysis of the key methods discussed in the literature, highlighting their features, advantages, limitations, and performance. This analysis demonstrates the efficiency of the proposed ERCO-Net method compared to existing approaches

III. EDGE RESTRICTION AND CONTEXTUAL OPTIMIZATION

Edge restriction in image processing is closely related to using spatial information, where certain attention is paid to edges and contours of images as needed [45], [46]. It also emphasizes the importance of providing margins and other small details in various image enhancements. More specifically, in the dehazing model, the boundary constraints must be applied to enhance the accuracy of estimates of the transmission map. This map is particularly useful when wanting to determine the extent of the haze that may be obscuring parts of the image [47], [48].

The core concept of the method entails controlling the dehazing operation based on understanding the type of change between objects or parts in the scene. It is mostly represented in equation form as a regularizer added to the energy function within the dehazing algorithm. Due to the priority given to edges and boundaries, the given algorithm risks receiving an infested image that lacks most of its necessary details while at the same time maintaining the clean image as natural as possible.

A. Working of Edge Restriction

The downsizing of the edges in the ERCO-Net is a significant component of the enhanced procedure. Because the transmission map would be required to estimate the edges of the objects, enhance edge preservation by the dehazing algorithm would be necessary [1]. Through the assignment of boundary constraints, the algorithm takes advantage of spatial information to improve the accuracy of the regression equations for the estimation of transmission map. Mathematically, this can be expressed in the following equation:

$$E_{\text{boundary}} = \lambda_b \int \|\nabla I - \nabla J\|^2 \, dx \tag{1}$$

In this context, E_{boundary} denotes the energy associated with boundary constraints. The variable I represents the hazy input image, J stands for the resulting dehazed image, and λ_b is a parameter that weights the boundary constraints appropriately.

B. Contextual Optimization in Dehazing

Contextual Optimization is the another prominent feature of the given approach which is crucial to be considered. It should resolve the issue of enhancing the dehazing process using contextual data at similar effectiveness. Contextual Optimization tends to enhance the neighboring pixels' coherency in an image thus enhancing the quality of the dehazed image [4]. Mathematically, it can be formulated as:

$$E_{\text{context}} = \lambda_c \int \|\nabla^2 J\|^2 \, dx \tag{2}$$

In this context, E_{context} denotes the energy associated with contextual optimization. The variable J represents the dehazed image, and λ_c is a parameter that optimizes this process.

By integrating edge restriction and contextual optimization, ERCO-Net aims to advance single-image dehazing techniques, providing a more robust solution to the challenges posed by atmospheric haze.

The flow of ERCO-Net is illustrated in Fig. 2.

ERCO-Net brings three key improvements. Firstly, introduce a new rule for how light travels through a scene. This rule is straightforward and easy to understand, and it turns out to be remarkably effective in clearing up hazy images. Secondly, introduce a new way to smooth out images by using a set of filters. These filters not only reduce unwanted noise in the images but also make certain features, like sudden changes and corners, stand out more. Lastly, a faster method has been developed to clean up large images, allowing for

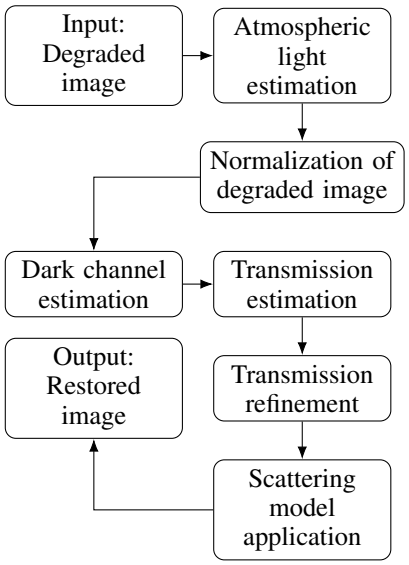

Fig. 2. Flowchart of the ERCO-Net dehazing process.

quick improvements in image clarity without taking much time.

The haze in the image is represented formally in a number of noteworthy work reported in [44], [49], [50], [51], depicted as follows:

$$Img(x) = st(x)R(x) + (1 - st(x))At \tag{3}$$

where, $Img(x)$ is the observed image, $R(x)$ is the scene radiance, At is the global atmospheric light, and $st(x)$ is the scene transmission. It is worthy to mention that the transmission function $st(x) : (0 \leq st(x) \leq 1)$ is related to the image depth.

The key objective of the image dehazing is to recover the image radiance $R(x)$ from $Img(x)$ based on Eq. 3. This requires us to estimate the transmission function $st(x)$ and the global atmospheric light At. Once $st(x)$ and At are estimated, the scene radiance can be recovered by:

$$R(x) = \frac{Img(x) - At}{[\max(st(x), \epsilon)]^{\lambda}} + At \tag{4}$$

IV. Edge Restriction from Radiance Cube

The concept of Boundary Constraint from Radiance Cube is a critical aspect in the context of image dehazing. The Radiance Cube represents the radiance values at different combinations of scene radiance and atmospheric light. The Boundary Constraint is employed to ensure that the estimated radiance values are constrained within physically meaningful bounds. In the context of image dehazing, this helps in preventing unrealistic or exaggerated scene radiance estimations.

- Atmospheric Light Constraint: The atmospheric light (A_t) is constrained to be within the range of 0 to 1. $0 \leq A_t \leq 1$
- Scene Radiance Constraint:
  The estimated scene radiance ($R(x)$) should be non-negative. $R(x) \geq 0$
- Transmission Constraint:
  The transmission ($st(x)$) lies between 0 and 1. $0 \leq st(x) \leq 1$
  4. Radiance Cube Constraint:
  The radiance cube values should be within a valid radiometric range.
  $L_{\text{min}} \leq L(x, \lambda) \leq L_{\text{max}}$
  Here, L_{min} and L_{max} represent the minimum and maximum radiance values, respectively.
- Boundary Constraint Equation:
  Combining the above constraints into a comprehensive boundary constraint equation:

$$R(x) = \frac{Img(x) - A_t}{[\max(st(x), \epsilon)]^{\lambda} + A_t} \tag{5}$$

This equation ensures that the estimated scene radiance ($R(x)$) is computed within the physically plausible boundaries while considering atmospheric light, transmission, and the Radiance Cube constraints.

These equations collectively enforce the Boundary Constraint, contributing to more realistic and physically meaningful results in the context of image dehazing. Adjustments to the parameters (ϵ and λ) may be made based on specific dehazing algorithms and requirements.

The above calculations can be depicted in Fig. 3.

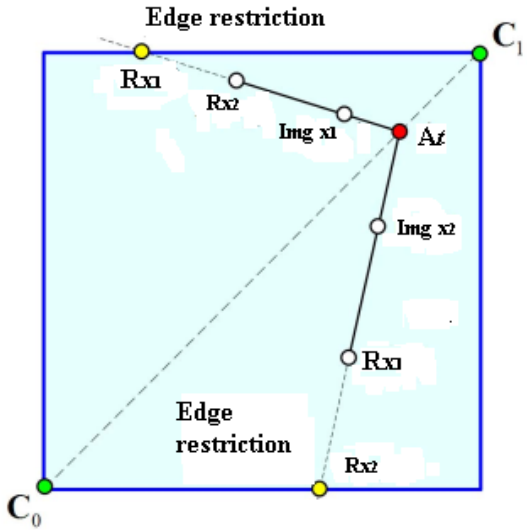

Fig. 3. A cube with boundary limitations that emits light. For every value of x, it is essential that the estimation of $J(x)$ does not surpass the limits of the radiance cube. $J_b(x_1)$ and $J_b(x_2)$ denote the precise positions that define the boundary constraints.

In geometric terms, as described by Eq. 3, when fog affects a pixel $Img(x)$, it tends to shift closer to the overall atmospheric light A_t, as illustrated in Fig. 3. Consequently, this effect can be counteracted by reversing the process and restoring the original clarity of the pixel, denoted as $R(x)$, through a linear extrapolation from A_t to Img_x. The extent of this extrapolation is determined as follows:

$$\frac{1}{st(x)} = \frac{|R(x) - A_t|}{|Img(x) - A_t|} \tag{6}$$

Let us contemplate the notion that the radiance of the scene within a particular image remains constrained; that is to say

$$C_0 \leq R(x) \leq C_1, \quad \forall x \in \Omega \tag{7}$$

In the context of the provided image, two constant vectors, C_0 and C_1, hold significance. Thus, it is imperative that for any given value of *x*, the extrapolation of $Rx)$ should fall within the radiance cube delineated by C_0 and C_1, as depicted in Fig. 3.

The requirement stated above for $R(x)$ leads to an edge restriction on $st(x)$. Assuming the global atmospheric light A_t is provided, the respective boundary constraint point $R(x_1)$ can be calculated for each *x* (see Fig. 3). Consequently, utilizing Eq. 6 and Eq. 7, a minimum value for $st(x)$ can be established, thereby setting the boundary constraint on $st(x)$ as follows:

$$0 \leq st_b(x) \leq st(x) \leq 1 \tag{8}$$

where $st_b(x)$ is the lower bound of $st(x)$, given by

$$st_b(x) = \min \left\{ \max_{c \in \{r,g,b\}} \left(\frac{A_t^c - \text{Img}(x)^c}{A_t^c - C_0^c}, \frac{A_t^c - \text{Img}(x)^c}{A_t^c - C_1^c} \right), 1 \right\} \tag{9}$$

here $Img(x)^c$, ${A_t}^c$, C_0^c and C_1^c are the color channels of $Img(x)$, A_t, C_0 and C_1, respectively

The edge constraint imposed by $st(x)$ provides a novel geometric viewpoint on the well-known dark channel prior [44]. Let's assign $C_0 = 0$ and suppose that the total atmospheric light A_t is brighter than any pixel in the foggy image. This enables us to compute $st_b(x)$ directly using Eq. 3, under the assumption that the dark channel of $R(x)$ at each pixel is zero. In addition, by assuming that the transmission remains constant inside a local image patch, the transmission for each patch $t\ddot{E}IJ(x)$ can be easily calculated using the method described in [44]. This is achieved by applying maximum filtering on $st_b(x)$ using Eq. 10.

$$\tilde{st}(x) = \max_{y \in \omega_x} st_b(y) \tag{10}$$

here ω_x is a local value being originated at *x*.

It is noteworthy that the edge restriction holds greater significance. In general, the ideal global atmospheric light is usually less bright than the brightest pixels in an image. These pixels often come from prominent light sources in the environment, like a brilliant sky or automobile headlights. While the dark channel prior may not effectively capture these bright pixels, the proposed edge restriction remains relevant.

Furthermore, it is of key importance that the commonly utilized constant assumption regarding transmission within a local image patch can be quite stringent. Consequently, the patch-wise transmission, as proposed in [44], [52] based on this assumption, is frequently undervalued. In this context, a more precise patch-wise transmission method is introduced that loosens the aforementioned assumption, thereby permitting slight variations in transmissions within a local patch. Eq. 11 depicts the formation of new patch-wise transformation:

$$\tilde{st}(x) = \min_{y \in \omega_x} \max_{z \in \omega_y} st_b(z) \tag{11}$$

The patch-wise transmission $\tilde{st}(x)$ can be efficiently calculated by simply applying a morphological closing operation on $st_b(x)$. Fig. 4 shows a comparison of the dehazing results achieved by using patch-wise transmissions derived from both the dark channel prior and the boundary constraint map. It is clear that the transmission derived from the dark channel prior is less effective in areas with bright sky. Furthermore, the dehazing results display noticeable halo artifacts.

Fig. 4. Results of image dehazing by applying patch-wise transmission from dark-channel and ERCO-Net (edge restriction). (a) The foggy image, (b) output dehazed image by dark-channel, (c) dehazing result be edge restriction.

A. Contextual Regularization based on L1-norm

Typically, pixels within a localized section of an image exhibit comparable depth values. Leveraging this presumption, a transmission method based on patch-wise constraints has been formulated. Nevertheless, this contextual inference frequently proves inadequate for image sections characterized by sudden depth changes, resulting in pronounced halo artifacts in the dehazing outcomes. This issue can be resolved by computing a weighting function wt on the edge restrictions, given below in Eq. 12.

$$wt(x, y)(st(y) - st(x)) \approx 0 \tag{12}$$

In the context of image processing, the relationship between adjacent pixels, denoted as *x* and *y*, is influenced by a weighting function. This function acts as a sort of "switch" determining the constraint between these pixels. Specifically, when the weighting function, $wt(x, y)$, equals zero, it effectively nullifies the contextual constraint of $st(x)$ between *x* and *y*. The suitable value of $wt(x, y)$ was determined to be inversely proportional to the difference between the values of *x* and *y*; i.e. the larger the distance between *x* and *y*, the lower the weight value. Additionally, it was determined that depth jumps primarily occur at the boundaries of images and within localized areas (or patches), where pixels of similar colors are likely to possess comparable depth values. This suggests that color variation among neighboring pixels can be calculated to create a weighting function. Two instances are provided to

demonstrate the formulation of such weighting functions. One approach entails computing the squared discrepancy between the color vectors of adjacent pixels, as seen in Eq. 13.

$$wt(x,y) = \frac{e^{-|Img(x)-Img(y)|^2}}{2\sigma^2} \tag{13}$$

Here σ acts as tune-able parameter. Same calculation is computed by considering (in Eq. 14) the difference in luminance of the neighboring pixels.

$$wt(x,y) = ((|lum(x) - lum(y)|)^{\alpha} + \epsilon)^{-1} \tag{14}$$

In this context, lum(x) refers to the logarithmic luminance channel of the image Img(x). The exponent $\alpha \geq 0$ determines the level of sensitivity to differences in luminance between two pixels, while ϵ is a small constant (typically 0.0001) used to prevent division by zero. The integration of the weighted contexts throughout the entire image leads to the subsequent contextual optimisation for $st(x)$:

$$\sum_{i \in I} \sum_{j \in \omega_i} wt_{ij} |st_i - st_j| \tag{15}$$

Here *I* is the index set of image pixels, wt_{ij} is the discrete versions of $wt(x,y)$.

B. Estimation of Scene Transmission

In image dehazing, estimating the scene transmission is a crucial step to recover the haze-free image from a hazy input. The scene transmission, denoted by $st(x)$, represents the proportion of light that is transmitted through the atmospheric medium at each pixel x in the image. A common model used for estimating scene transmission is the dark channel prior (DCP) proposed by [44].

The dark channel prior exploits the statistical property that in most outdoor natural images, there exist some pixels with very low intensity values in at least one color channel. This property holds true even in hazy images.

The dark channel $J^{dark}(x)$ of an image J is defined as:

$$J^{dark}(x) = \min_{y \in \Omega(x)} (\min_{c \in \{r,g,b\}} (J^c(y))) \tag{16}$$

where $J^c(y)$ represents the intensity of channel c at pixel y, and $\Omega(x)$ is a local patch centered at pixel x.

The scene transmission $t(x)$ can then be estimated using the dark channel prior as:

$$t(x) = 1 - \omega \cdot \min_{y \in \Omega(x)} (J^{dark}(y)) \tag{17}$$

where ω is a small positive constant used to control the amount of haze removal.

By utilizing the dark channel prior to estimate the scene transmission, the areas of the image impacted by haze can be accurately detected and their intensity appropriately reduced throughout the dehazing procedure.

V. Results with Discussion

Fig. 5 depicts the process of scene transformation estimation of the image performed in different iterations, by applying Eq. 16 and Eq.17.

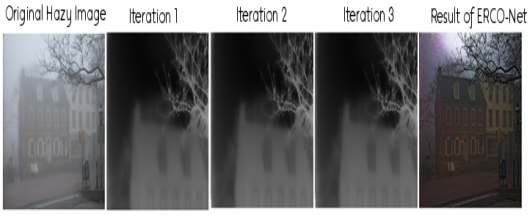

Fig. 5. Results of applying scene transmission estimation on hazy image. The results are shown in iteration followed by the final output.

The results are generated by adjusting the value of *w* to 0.5 in Eq. 17. The edge restriction is set to the C_0 to $(20, 10, 20)^T$ and C_1 to $(150, 150, 300)^T$ in Eq. 9. These adjustments assist in adjusting the haze map with in the view-able window.

The results demonstrate ERCO-Net ability to effectively restore intricate details and vibrant color information within hazy regions of images. It's important to emphasize that the estimated transmissions displayed in the three images on the right side of the figure are not merely scaled versions of depth maps. This is due to the non-uniform distribution of haze across these images, particularly evident in image featuring expansive clear sky areas. Essentially, the transmission function serves as a reflection of the haze density present within the captured image, rather than simply representing depth.

A. Comparison with Other Approaches

For evaluation purposes, the ERCO-Net results were also compared with some state-of-the-art models. These models include dark channel prior (DCP) [44], Atmospheric Light Estimation (ALT) [53], Image Fusion [54], and multiscale retinex [55].

Fig. 6 depicts the comparison of our approach with the algorithms aforementioned.

Fig. 6. Comparison with DCP, ALT, Image Fusion, and MSR approaches using ERCO-Net on the NH-Haze2 dataset [56].

Similarly, Fig. 7 shows the output of our algorithm in comparison with other models.

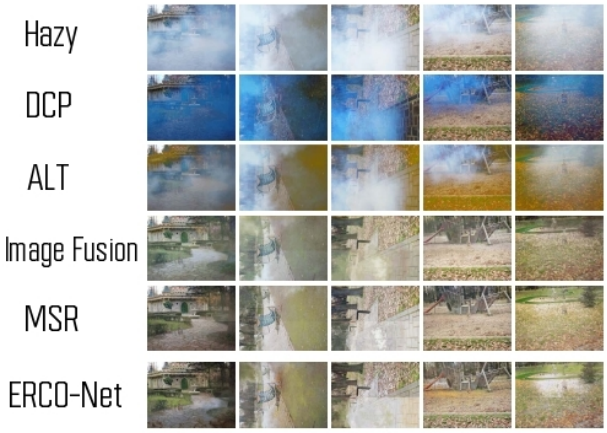

Fig. 7. Comparison with DCP, ALT, Image Fusion, and MSR approaches using ERCO-Net on the NH-Haze2 dataset [57].

For evaluation purposes, two metrics are employed: the Structural Similarity Index (SSIM) and the Peak Signal-to-Noise Ratio (PSNR). These metrics are frequently utilized in image processing to evaluate the quality of images.

Table II presents the comparison of our approach with other algorithms over NHHaze and NHHaze-2 datasets.

TABLE II. QUANTITATIVE COMPARISONS OVER NHHAZE AND NHHAZE-2 DATASETS FOR DIFFERENT METHODS AND ERCO-NET APPROACH

Methods	NHHaze		NHHaze2	
	PSNR	SSIM	PSNR	SSIM
DCP	16.62	0.817	12.92	0.505
ALT	19.06	0.85	17.69	0.616
Image fusion	30.23	0.975	19.5	0.66
MSR	34.59	0.975	23.53	0.754
ERCO-Net	**37.61**	**0.991**	**25.54**	**0.783**

VI. CONCLUSION

In the field of single image dehazing, a significant challenge arises from the inherent ambiguity between image color and depth. This ambiguity often leads to difficulty in distinguishing between haze-affected and unaffected pixels, particularly when their coloration is similar. ERCO-Net addresses this challenge by combining edge restriction and contextual optimization, which improves image clarity and preserves critical details. The method demonstrated reliable dehazing performance with reduced computational complexity, highlighting its potential for practical applications. Future work will focus on further optimizing ERCO-Net for large-scale datasets and addressing limitations in extreme haze conditions. Additionally, improvements in edge detail retention and the exploration of its applicability to other image restoration tasks will be key areas of investigation.

ACKNOWLEDGMENT

We would like to express sincere gratitude to AlMaarefa University, Riyadh, Saudi Arabia, for supporting this research.

DECLARATIONS

Conflicts of Interests / Competing Interests

The authors declare that they have no conflict of interest.

REFERENCES

[1] B. Li, W. Ren, D. Fu, D. Tao, D. Feng, W. Zeng, and Z. Wang, "Benchmarking single-image dehazing and beyond," *IEEE Transactions on Image Processing*, vol. 28, no. 1, pp. 492–505, 2018.

[2] H. Wu, Y. Qu, S. Lin, J. Zhou, R. Qiao, Z. Zhang, Y. Xie, and L. Ma, "Contrastive learning for compact single image dehazing," in *Proceedings of the IEEE/CVF Conference on Computer Vision and Pattern Recognition*, 2021, pp. 10 551–10 560.

[3] L. Li, Y. Dong, W. Ren, J. Pan, C. Gao, N. Sang, and M.-H. Yang, "Semi-supervised image dehazing," *IEEE Transactions on Image Processing*, vol. 29, pp. 2766–2779, 2019.

[4] A. Golts, D. Freedman, and M. Elad, "Unsupervised single image dehazing using dark channel prior loss," *IEEE transactions on Image Processing*, vol. 29, pp. 2692–2701, 2019.

[5] Z. Zhu, Y. Luo, H. Wei, Y. Li, G. Qi, N. Mazur, Y. Li, and P. Li, "Atmospheric light estimation based remote sensing image dehazing," *Remote Sensing*, vol. 13, no. 13, p. 2432, 2021.

[6] S. C. Agrawal and A. S. Jalal, "A comprehensive review on analysis and implementation of recent image dehazing methods," *Archives of Computational Methods in Engineering*, vol. 29, no. 7, pp. 4799–4850, 2022.

[7] Y. Song, Z. He, H. Qian, and X. Du, "Vision transformers for single image dehazing," *IEEE Transactions on Image Processing*, vol. 32, pp. 1927–1941, 2023.

[8] B. Li, X. Peng, Z. Wang, J. Xu, and D. Feng, "Aod-net: All-in-one dehazing network," in *Proceedings of the IEEE international conference on computer vision*, 2017, pp. 4770–4778.

[9] W. Ren, J. Pan, H. Zhang, X. Cao, and M.-H. Yang, "Single image dehazing via multi-scale convolutional neural networks with holistic edges," *International Journal of Computer Vision*, vol. 128, pp. 240–259, 2020.

[10] P. Sharma, P. Jain, and A. Sur, "Scale-aware conditional generative adversarial network for image dehazing," in *Proceedings of the IEEE/CVF Winter Conference on Applications of Computer Vision*, 2020, pp. 2355–2365.

[11] X. Zhang, T. Wang, J. Wang, G. Tang, and L. Zhao, "Pyramid channel-based feature attention network for image dehazing," *Computer Vision and Image Understanding*, vol. 197, p. 103003, 2020.

[12] D. Chen, M. He, Q. Fan, J. Liao, L. Zhang, D. Hou, L. Yuan, and G. Hua, "Gated context aggregation network for image dehazing and deraining," in *2019 IEEE winter conference on applications of computer vision (WACV)*. IEEE, 2019, pp. 1375–1383.

[13] Y.-W. Lee, L.-K. Wong, and J. See, "Image dehazing with contextualized attentive u-net," in *2020 IEEE International Conference on Image Processing (ICIP)*. IEEE, 2020, pp. 1068–1072.

[14] L. Yan, W. Zheng, C. Gou, and F.-Y. Wang, "Feature aggregation attention network for single image dehazing," in *2020 IEEE International Conference on Image Processing (ICIP)*. IEEE, 2020, pp. 923–927.

[15] S. Zhang and F. He, "Drcdn: learning deep residual convolutional dehazing networks," *The Visual Computer*, vol. 36, no. 9, pp. 1797–1808, 2020.

[16] S. Zhang, F. He, and W. Ren, "Photo-realistic dehazing via contextual generative adversarial networks," *Machine Vision and Applications*, vol. 31, no. 5, p. 33, 2020.

[17] A. Dudhane, H. Singh Aulakh, and S. Murala, "Ri-gan: An end-to-end network for single image haze removal," in *Proceedings of the IEEE/CVF conference on computer vision and pattern recognition workshops*, 2019, pp. 0–0.

[18] G. Tang, L. Zhao, R. Jiang, and X. Zhang, "Single image dehazing via lightweight multi-scale networks," in *2019 IEEE International Conference on Big Data (Big Data)*. IEEE, 2019, pp. 5062–5069.

[19] A. Wang, W. Wang, J. Liu, and N. Gu, "Aipnet: Image-to-image single image dehazing with atmospheric illumination prior," *IEEE Transactions on Image Processing*, vol. 28, no. 1, pp. 381–393, 2018.

[20] C. Wang, Y. Zou, and Z. Chen, "Abc-net: Avoiding blocking effect & color shift network for single image dehazing via restraining transmission bias," in *2020 IEEE International Conference on Image Processing (ICIP)*. IEEE, 2020, pp. 1053–1057.

[21] S. Chen, Y. Chen, Y. Qu, J. Huang, and M. Hong, "Multi-scale adaptive dehazing network," in *Proceedings of the IEEE/CVF conference on computer vision and pattern recognition workshops*, 2019, pp. 0–0.

[22] A. Singh, A. Bhave, and D. K. Prasad, "Single image dehazing for a variety of haze scenarios using back projected pyramid network," in *Computer Vision–ECCV 2020 Workshops: Glasgow, UK, August 23–28, 2020, Proceedings, Part IV 16*. Springer, 2020, pp. 166–181.

[23] S. Yin, Y. Wang, and Y.-H. Yang, "A novel image-dehazing network with a parallel attention block," *Pattern Recognition*, vol. 102, p. 107255, 2020.

[24] H. Zhang and V. M. Patel, "Densely connected pyramid dehazing network," in *Proceedings of the IEEE conference on computer vision and pattern recognition*, 2018, pp. 3194–3203.

[25] H. Zhang, V. Sindagi, and V. M. Patel, "Multi-scale single image dehazing using perceptual pyramid deep network," in *Proceedings of the IEEE conference on computer vision and pattern recognition workshops*, 2018, pp. 902–911.

[26] D. Zhao, L. Xu, L. Ma, J. Li, and Y. Yan, "Pyramid global context network for image dehazing," *IEEE Transactions on Circuits and Systems for Video Technology*, vol. 31, no. 8, pp. 3037–3050, 2020.

[27] C.-L. Guo, Q. Yan, S. Anwar, R. Cong, W. Ren, and C. Li, "Image dehazing transformer with transmission-aware 3d position embedding," in *Proceedings of the IEEE/CVF conference on computer vision and pattern recognition*, 2022, pp. 5812–5820.

[28] X. Chen, H. Lu, K. Cheng, Y. Ma, Q. Zhou, and Y. Zhao, "Sequentially refined spatial and channel-wise feature aggregation in encoder-decoder network for single image dehazing," in *2019 IEEE International Conference on Image Processing (ICIP)*. IEEE, 2019, pp. 2776–2780.

[29] M. Hong, Y. Xie, C. Li, and Y. Qu, "Distilling image dehazing with heterogeneous task imitation," in *Proceedings of the IEEE/CVF conference on computer vision and pattern recognition*, 2020, pp. 3462–3471.

[30] X. Liang, R. Li, and J. Tang, "Selective attention network for image dehazing and deraining," in *Proceedings of the 1st ACM International Conference on Multimedia in Asia*, 2019, pp. 1–6.

[31] Y. Qu, Y. Chen, J. Huang, and Y. Xie, "Enhanced pix2pix dehazing network," in *Proceedings of the IEEE/CVF conference on computer vision and pattern recognition*, 2019, pp. 8160–8168.

[32] Z. Zhang, L. Zhao, Y. Liu, S. Zhang, and J. Yang, "Unified density-aware image dehazing and object detection in real-world hazy scenes," in *Proceedings of the Asian Conference on Computer Vision*, 2020.

[33] R. Chen and E. M.-K. Lai, "Convolutional autoencoder for single image dehazing." in *ICIP*, 2019, pp. 4464–4468.

[34] Y. Dong, Y. Liu, H. Zhang, S. Chen, and Y. Qiao, "Fd-gan: Generative adversarial networks with fusion-discriminator for single image dehazing," in *Proceedings of the AAAI Conference on Artificial Intelligence*, vol. 34, no. 07, 2020, pp. 10 729–10 736.

[35] H. Zhu, X. Peng, V. Chandrasekhar, L. Li, and J.-H. Lim, "Dehazegan: When image dehazing meets differential programming." in *IJCAI*, 2018, pp. 1234–1240.

[36] F. Yang and Q. Zhang, "Depth aware image dehazing," *The Visual Computer*, vol. 38, no. 5, pp. 1579–1587, 2022.

[37] H. Dong, X. Zhang, Y. Guo, and F. Wang, "Deep multi-scale gabor wavelet network for image restoration," in *ICASSP 2020-2020 IEEE International Conference on Acoustics, Speech and Signal Processing (ICASSP)*. IEEE, 2020, pp. 2028–2032.

[38] X. Liu, Y. Ma, Z. Shi, and J. Chen, "Griddehazenet: Attention-based multi-scale network for image dehazing," in *Proceedings of the IEEE/CVF international conference on computer vision*, 2019, pp. 7314–7323.

[39] K. Metwaly, X. Li, T. Guo, and V. Monga, "Nonlocal channel attention for nonhomogeneous image dehazing," in *Proceedings of the IEEE/CVF conference on computer vision and pattern recognition workshops*, 2020, pp. 452–453.

[40] X. Qin, Z. Wang, Y. Bai, X. Xie, and H. Jia, "Ffa-net: Feature fusion attention network for single image dehazing," in *Proceedings of the AAAI conference on artificial intelligence*, vol. 34, no. 07, 2020, pp. 11 908–11 915.

[41] J. Wang, C. Li, and S. Xu, "An ensemble multi-scale residual attention network (emra-net) for image dehazing," *Multimedia Tools and Applications*, vol. 80, no. 19, pp. 29 299–29 319, 2021.

[42] S. Yin, X. Yang, Y. Wang, and Y.-H. Yang, "Visual attention dehazing network with multi-level features refinement and fusion," *Pattern Recognition*, vol. 118, p. 108021, 2021.

[43] P. Shyam and H. Yoo, "Data efficient single image dehazing via adversarial auto-augmentation and extended atmospheric scattering model," in *Proceedings of the IEEE/CVF International Conference on Computer Vision*, 2023, pp. 227–237.

[44] K. He, J. Sun, and X. Tang, "Single image haze removal using dark channel prior," *IEEE transactions on pattern analysis and machine intelligence*, vol. 33, no. 12, pp. 2341–2353, 2010.

[45] L. Chen, W. Wu, C. Fu, X. Han, and Y. Zhang, "Weakly supervised semantic segmentation with boundary exploration," in *Computer Vision–ECCV 2020: 16th European Conference, Glasgow, UK, August 23–28, 2020, Proceedings, Part XXVI 16*. Springer, 2020, pp. 347–362.

[46] Y. Liu, J. Pan, J. Ren, and Z. Su, "Learning deep priors for image dehazing," in *Proceedings of the IEEE/CVF international conference on computer vision*, 2019, pp. 2492–2500.

[47] J. Wan, Z. Lai, J. Li, J. Zhou, and C. Gao, "Robust facial landmark detection by multiorder multiconstraint deep networks," *IEEE Transactions on Neural Networks and Learning Systems*, vol. 33, no. 5, pp. 2181–2194, 2021.

[48] D. Yang and J. Sun, "Proximal dehaze-net: A prior learning-based deep network for single image dehazing," in *Proceedings of the european conference on computer vision (ECCV)*, 2018, pp. 702–717.

[49] R. Fattal, "Single image dehazing," *ACM transactions on graphics (TOG)*, vol. 27, no. 3, pp. 1–9, 2008.

[50] S. G. Narasimhan and S. K. Nayar, "Contrast restoration of weather degraded images," *IEEE transactions on pattern analysis and machine intelligence*, vol. 25, no. 6, pp. 713–724, 2003.

[51] R. T. Tan, "Visibility in bad weather from a single image," in *2008 IEEE conference on computer vision and pattern recognition*. IEEE, 2008, pp. 1–8.

[52] W.-C. Cheng, H.-C. Hsiao, W.-L. Huang, and C.-H. Hsieh, "Image haze removal using dark channel prior technology with adaptive mask size." *Sensors & Materials*, vol. 32, 2020.

[53] H. Lu, Y. Li, S. Nakashima, and S. Serikawa, "Single image dehazing through improved atmospheric light estimation," *Multimedia Tools and Applications*, vol. 75, pp. 17 081–17 096, 2016.

[54] Z. Zhu, H. Wei, G. Hu, Y. Li, G. Qi, and N. Mazur, "A novel fast single image dehazing algorithm based on artificial multiexposure image fusion," *IEEE Transactions on Instrumentation and Measurement*, vol. 70, pp. 1–23, 2020.

[55] J. Wang, K. Lu, J. Xue, N. He, and L. Shao, "Single image dehazing based on the physical model and msrcr algorithm," *IEEE Transactions on Circuits and Systems for Video Technology*, vol. 28, no. 9, pp. 2190–2199, 2017.

[56] C. O. Ancuti, C. Ancuti, F.-A. Vasluianu, and R. Timofte, "Ntire 2021 nonhomogeneous dehazing challenge report," in *Proceedings of the IEEE/CVF Conference on Computer Vision and Pattern Recognition*, 2021, pp. 627–646.

[57] C. O. Ancuti, C. Ancuti, and R. Timofte, "Nh-haze: An image dehazing benchmark with non-homogeneous hazy and haze-free images," in *Proceedings of the IEEE/CVF conference on computer vision and pattern recognition workshops*, 2020, pp. 444–445.